Single-photon router: Coherent control of multichannel scattering for single photons with quantum interferences

Jing Lu (卢竞),[1,2] Lan Zhou (周兰),[1,3,*] Le-Man Kuang (匡乐满),[1] and Franco Nori (野理)[2,4]

[1]*Key Laboratory of Low-Dimensional Quantum Structures and Quantum Control of Ministry of Education
and Department of Physics, Hunan Normal University, Changsha 410081, China*
[2]*CEMS, RIKEN, Saitama 351-0198, Japan*
[3]*Beijing Computational Science Research Center, Beijing 100084, China*
[4]*Physics Department, The University of Michigan, Ann Arbor, Michigan 48109-1040, USA*
(Received 12 November 2013; published 7 January 2014)

We propose a single-photon router using a single atom with an inversion center coupled to quantum multichannels made of coupled-resonator waveguides. We show that the spontaneous emission of the atom can direct single photons from one quantum channel into another. The on-demand classical field perfectly switches off the single-photon routing due to the quantum interference in the atomic amplitudes of optical transitions. Total reflections in the incident channel are due to the photonic bound state in the continuum. Two virtual channels, named the scatter-free and controllable channels, are found, which are coherent superpositions of quantum channels. Any incident photon in the scatter-free channel is totally transmitted. The propagating states of the controllable channel are orthogonal to those of the scatter-free channel. Single photons in the controllable channel can be perfectly reflected or transmitted by the atom.

PACS number(s): 42.50.Pq, 42.50.Ex, 03.67.Lx, 78.67.−n

I. INTRODUCTION

A quantum network [1] consists of quantum channels and nodes, which are provided by waveguides and quantum emitters, respectively. The flying qubits in quantum channels serve to distribute quantum information. The static qubits in local nodes generate, process, and route quantum information. Photons are ideal carriers in quantum channels because they are fast, robust, and readily available. Although it is easy to control photons in linear optical systems [2–5], waveguides are more promising, as the technology proceeds to smaller on chip structures. Currently, considerable attention has been paid to photon transport in one-dimensional (1D) waveguides with a quantum emitter both in theory [6–22] and in experiments [23–30]. The waveguide confines photons in low dimensions and has a dispersion relation different from photons in free space, giving rise to new physical phenomena, e.g., the total reflection in Refs. [6] and [7]. The coupled-resonator waveguide (CRW) [31] is an important waveguide for studying waveguide QED due to the following advantages: (1) strong coupling between light and matter; (2) wider bandwidths; (3) scalability (e.g., ultrahigh-Q coupled nanocavity arrays with $N > 100$ have been realized in photonic crystals [32]); (4) easy addressability; and (5) ability to simulate the behavior of single particles in the short- and long-wavelength regimes. The discreteness of CRW offers a rich variety of properties and possibilities that do not exist in the bulk, e.g., bound states outside the band [33]. Currently, many photonic devices (see, e.g., [7–11], and references therein) based on using single atoms in a 1D CRW have been proposed. Most of the theoretical work focuses on controlling photons in one continuum of propagating states. Recently, a cyclic three-level system embedded in multiple quantum channels formed with 1D CRWs has been proposed as a quantum router [9], where single photons are routed from one continuum to another by the cyclic system with the help of a classical control field. However, the experimental realization of this proposal faces the challenge that cyclic transitions are forbidden for natural atoms, as these possess an inversion center [34]. One should use either chiral systems [35] or atoms whose symmetry is broken artificially [36,37]. These bring complexities to a possible realization. A router using natural atoms will certainly contribute to the studies on quantum networks and routers and facilitate their experimental realization.

In this work, we propose a single-photon routing scheme using systems with an inversion center. The two continua of propagating states are constructed by two 1D CRWs. To control the transfer of propagating states from one continuum to the other, we explore quantum coherence and interference effects, such as the electromagnetically induced transparency in a system of a three-level Λ atom embedded inside the two 1D CRWs. Here the Λ atom plays the role of a quantum node for routing. One transition of the Λ atom is coupled to the photonic modes of two CRWs. The other transition is driven by a classical field. Differently from the routers [38,39] based on designing a time-dependent classical field acting on a large area of the considered system, here, a classical field is applied to individually address the atom. The scattering process is studied when a single photon is incident from one CRW. We find that the quantum node indeed works as a multichannel quantum router, and the classical field selects the channel to which single photons are directed or transferred. The multichannel effect is taken into account by studying the single-photon scattering process with waves incident from two CRWs. A controllable channel and a scattering-free channel [13] are found when both CRWs are identical.

This paper is organized as follows: In Sec. II, we introduce our model, which consists of a three-level Λ atom embedded in two CRWs. In Sec. III, we employ the discrete-coordinate scattering approach to study the scattering process of single photons and give the expressions for scattering amplitudes. We

*Corresponding author: zzhoulan@gmail.com

discuss the function of the three-level atom in Sec. IV using the eigenstates for the total system. Here, two band configurations of the two CRWs are studied, and the underlying physics for controlling single-photon routing are discussed. In Sec. V, we study the possibility of a three-level atom acting as a perfect mirror or a transparent medium for single photons with waves incident from two CRWs. Finally, we conclude with a brief summary of the results, with accompanying discussion.

II. MODEL SETUP

As shown in Fig. 1, our hybrid system consists of two 1D CRWs and a three-level system. The cavity modes of the two 1D CRWs are described by the annihilation operators a_j and b_j, respectively, and subscript $j = -\infty, \ldots, +\infty$. The atom located at $j = 0$ is characterized by the ground state $|g\rangle$, one intermediate state $|s\rangle$, and an excited state $|e\rangle$. The transition $|g\rangle \leftrightarrow |e\rangle$ is dipole-coupled to the cavity modes a_0 and b_0, with coupling strengths g_a and g_b, respectively. Obviously, the cavity-driven transition builds a bridge between these two CRWs. A classical field with frequency ν drives the atomic transition $|s\rangle \leftrightarrow |e\rangle$ with Rabi frequency Ω. The transition between the ground and the intermediate states is forbidden.

Once a photon is inside one cavity of the CRW, it propagates along the CRW and is also scattered by the atoms. The total Hamiltonian of this hybrid system $H = H_C + H_A' + H_{CA}$ contains three parts: The Hamiltonian H_C describes the two CRWs, H_A' is the free Hamiltonian of the Λ-type three-level atom, and H_{CA} describes the interactions among the cavity modes, the classical field, and the atom. The two CRWs are modeled as two independent linear chains of sites with a nearest-neighbor interaction, which are described by the Hamiltonian

$$H_C = \sum_j [\omega_a a_j^\dagger a_j - \xi_a(a_j^\dagger a_{j+1} + \text{H.c.})]$$
$$+ \sum_j [\omega_b b_j^\dagger b_j - \xi_b(b_j^\dagger b_{j+1} + \text{H.c.})]. \quad (1)$$

For simplicity, we assume that all resonators in CRW-a (CRW-b) have the same frequency ω_a (ω_b), and the hopping energies ξ_a (ξ_b) between any two nearest-neighbor cavities in CRW-a (CRW-b) are the same. By introducing the Fourier transform $d_k = \frac{1}{\sqrt{2\pi}} d_j e^{ik_d j}$, $d = a,b$, we see that each bare CRW supports plane waves with the dispersion relation

$$E_k^{[a]} = \omega_a - 2\xi_a \cos k_a, \quad (2a)$$

$$E_k^{[b]} = \omega_b - 2\xi_b \cos k_b, \quad (2b)$$

which indicates that each CRW possesses an energy band with bandwidth $4\xi_a$ and $4\xi_a$, respectively. Consequently, two continua are formed. In Fig. 1, all the resonators connected by the red (blue) line form photonic channel a (b), which is referred to as CRW-a (CRW-b) hereafter. We note that the central cavity with the atom comprises two cavities (see Fig. 1): one lies on the red line, which is described by the bosonic destruction operator a_0; the other lies on the green line, which
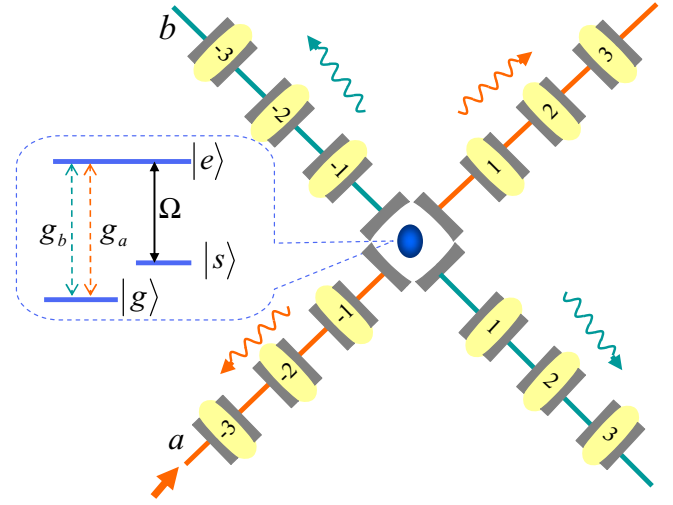

FIG. 1. (Color online) Schematic routing of single photons in two channels made of two CRWs. The three-level atom characterized by $|g\rangle$, $|e\rangle$, and $|s\rangle$ is placed at the cross point $j = 0$. CRW-a (CRW-b) couples to the atom through the transition $|g\rangle \leftrightarrow |e\rangle$ with strength g_a (g_b), and a classical field with Rabi frequency Ω is applied to drive the $|e\rangle \leftrightarrow |s\rangle$ transition. An incoming wave from the left side of the CRW-a will be reflected, transmitted, or transferred to the CRW-b.

is described by the bosonic destruction operator b_0. The Hamiltonian for the free Λ-type three-level atom reads

$$H_A' = \omega_E |e\rangle\langle e| + \omega_S' |s\rangle\langle s|, \quad (3)$$

where we have chosen the energy of the ground state $|g\rangle$ as the energy reference. The interaction Hamiltonian

$$H_{CA} = |e\rangle\langle g| (g_a a_0 + g_b b_0) + \Omega |e\rangle\langle s| e^{-i\nu t} + \text{H.c.} \quad (4)$$

is written under the rotating-wave approximation. We note here that the classical field only acts on the atom. To remove the time-dependent factor of the Hamiltonian, we rewrite the Hamiltonian in a rotating frame of reference, which is defined by the unitary transformation $U = \exp(i\nu t |s\rangle\langle s|)$. The Hamiltonian $H_R \equiv U^\dagger H U - i U^\dagger \partial_t U$ in this rotating frame still consists of three parts. The part for the CRWs remains the same. The free Λ-type atom transforms to

$$H_A = \omega_E |e\rangle\langle e| + \omega_S |s\rangle\langle s|, \quad (5)$$

where $\omega_S = \omega_S' + \nu$ is the frequency sum of the intermediate state and the classical light field. The time-dependent interaction Hamiltonian becomes

$$H_I = |e\rangle\langle g| (g_a a_0 + g_b b_0) + \Omega |e\rangle\langle s| + \text{H.c.}, \quad (6)$$

which is independent of time. Hereafter, we study the single-photon scattering in this rotating frame. We note that when a classical field is absent, i.e., $\Omega = 0$, this system becomes a two-level atom embedded in two CRWs.

III. COHERENT SCATTERING OF SINGLE PHOTONS

It can be found that the operator

$$N = \sum_j (a_j^\dagger a_j + b_j^\dagger b_j) + |e\rangle\langle e| + |s\rangle\langle s| \quad (7)$$

commutes with the Hamiltonian H_R. Since the number of quanta is conserved in this hybrid system, three mutually exclusive possibilities are involved in the one-quantum subspace: (i) The particle freely propagates in the two CRWs; (ii) the particle is absorbed by the atom, consequently, the atom is populated in its excited state; and (iii) the classical field stimulates the atom into its intermediate state. This implies the stationary eigenstate

$$|E\rangle = \sum_j \alpha(j) a_j^\dagger |g0\rangle + \sum_j \beta(j) b_j^\dagger |g0\rangle$$
$$+ u_e |e0\rangle + u_s |s0\rangle, \qquad (8)$$

where $|0\rangle$ is the vacuum state of the two CRWs. Here, $\alpha(j)$ and $\beta(j)$ are the probability amplitudes of single-photon states in the jth cavity of CRW-a and CRW-b, respectively. Also, u_e and u_s are the probability amplitudes of the three-level system in its excited and intermediate states, respectively.

The eigenequation gives rise to a series of coupled stationary equations for all amplitudes,

$$(E - \omega_E) u_e = \Omega u_s + g_a \alpha(0) + g_b \beta(0),$$
$$(E - \omega_S) u_s = \Omega^* u_e,$$
$$(E - \omega_a) \alpha(j) = -\xi_a [\alpha(j-1) + \alpha(j+1)] + \delta_{j0} g_a u_e,$$
$$(E - \omega_b) \beta(j) = -\xi_b [\beta(j-1) + \beta(j+1)] + \delta_{j0} g_b u_e,$$

where $\delta_{mn} = 1\ (0)$ for $m = n\ (m \neq n)$. Removing the atomic amplitudes in the above equation leads to the discrete-scattering equation of single photons,

$$(E - \omega_a)\alpha(j) = -\xi_a[\alpha(j-1) + \alpha(j+1)] + \delta_{j0}\alpha(j) V_a(E)$$
$$+ \delta_{j0}\beta(j) G(E), \qquad (9a)$$
$$(E - \omega_b)\beta(j) = -\xi_b[\beta(j-1) + \beta(j+1)] + \delta_{j0}\alpha(j) G(E)$$
$$+ \delta_{j0}\beta(j) V_b(E), \qquad (9b)$$

where we have introduced the energy-dependent δ-like potentials $V_d(E) \equiv g_d^2 V(E)$, with

$$V(E) \equiv \frac{(E - \omega_S)}{(E - \omega_E)(E - \omega_S) - |\Omega|^2}, \qquad (10)$$

and the effective dispersive coupling strength

$$G(E) \equiv g_a g_b V(E) \qquad (11)$$

between cavity mode a_0 and cavity mode b_0. It should be pointed out that the energy of the incident photon indirectly determines whether a repulsive or an attractive potential is localized at $j = 0$, as well as the magnitude of the δ-like potentials and effective coupling strengths. Since $V_d(E)$ and $G(E)$ are induced by the atom, we rewrite Eq. (10) as

$$V(E) = \frac{A_+}{E - \omega_+} + \frac{A_-}{E - \omega_-} \qquad (12)$$

to capture the effect of the atomic quantum interference, with frequencies $\omega_\pm = (\omega_S + \omega_E \pm \mu)/2$ and numerators $A_\pm = [1 \pm (\omega_E - \delta_S)\mu^{-1}]/2$ with

$$\mu = \sqrt{(\omega_E - \omega_S)^2 + 4|\Omega|^2}. \qquad (13)$$

A. Dressed states

Equation (12) indicates that a classical field dresses the atom to form doubly excited states with energies $\omega_\pm$ (called dressed states). The parameter μ denotes the energy splitting between the two dressed states. At $E = \omega_\pm$, infinite δ potentials are formed at $j = 0$ in both CRWs. It seems that the δ potential would prevent the propagation of single photons. However, the effective coupling strength $G(E)$ also becomes infinite at $E = \omega_\pm$, which may enable the transfer of the photon from one CRW to the other. When the energy of the incident photon satisfies the two-photon resonance condition $E = \omega_S$, both $V_d(E)$ and $G(E)$ vanish, and the two CRWs are decoupled. When the Rabi frequency $\Omega \to 0$, $\omega_+ \to \omega_E$ and $\omega_- \to \omega_S$. However, $A_+ \to 1$, $A_- \to 0$; i.e., our hybrid system becomes two CRWs coupled to a two-level system (TLS) in the absence of a classical field. Infinite δ potentials and an infinite effective coupling strength between the two CRWs can also be obtained when the energy of the incident photon is resonant with the TLS. Consequently, it is still possible for the photon to be transferred from one CRW to the other. However, it is impossible to decouple the two CRWs.

B. How the router works

An incident wave impinging upon the left side of one CRW (e.g., a) will result in reflected, transmitted, and transfer waves with the same energy. The wave functions in the asymptotic regions are given by

$$\alpha(j) = \begin{cases} e^{ik_a j} + r^a e^{-ik_a j}, & j < 0, \\ t^a e^{ik_a j}, & j > 0, \end{cases} \qquad (14a)$$

$$\beta(j) = \begin{cases} t_l^b e^{-ik_b j}, & j < 0, \\ t_r^b e^{ik_b j}, & j > 0, \end{cases} \qquad (14b)$$

where t^a (r^a) is the transmitted (reflected) amplitude and t_l^b (t_r^b) is the forward (backward) transfer amplitude. The relation $E = E_k^{[a]} = E_k^{[b]}$ between wavenumber k_a and wavenumber k_b can be obtained by applying Eq. (14) to the discrete scattering, Eq. (9), far away from the $j = 0$ site. However, applying Eq. (14) to the discrete scattering, Eq. (9), for the 0th and ± 1st sites, we obtain the continuity conditions $t_l^b = t_r^b \equiv t^b$ and $t^a = r^a + 1$, and the scattering amplitudes

$$t^a = \frac{2i\xi_a \sin k_a [2i\xi_b \sin k_b - V_b(E)]}{\prod_{d=a,b}[2i\xi_d \sin k_d - V_d(E)] - G^2(E)}, \qquad (15a)$$

$$t^b = \frac{G(E) 2i\xi_a \sin k_a}{\prod_{d=a,b}[2i\xi_d \sin k_d - V_d(E)] - G^2(E)}. \qquad (15b)$$

It can be observed that $t^a = 1$ at $E = \omega_S$, which means that the incident photon with energy $E = \omega_S$ will be totally transmitted in its original CRW due to the vanishing $V_d(E)$ and $G(E)$.

In Fig. 2, we plotted the transmittance $T^a(E) \equiv |t^a(E)|^2$, transfer rate $T^b \equiv |t^b(E)|^2$, and reflectance $R^a(E) \equiv |r^a(E)|^2$, as a function of the incident energy E, for three band configurations of the two bare CRWs. In Fig. 2(a), two bands of the CRWs are maximally overlapped. It can be seen that
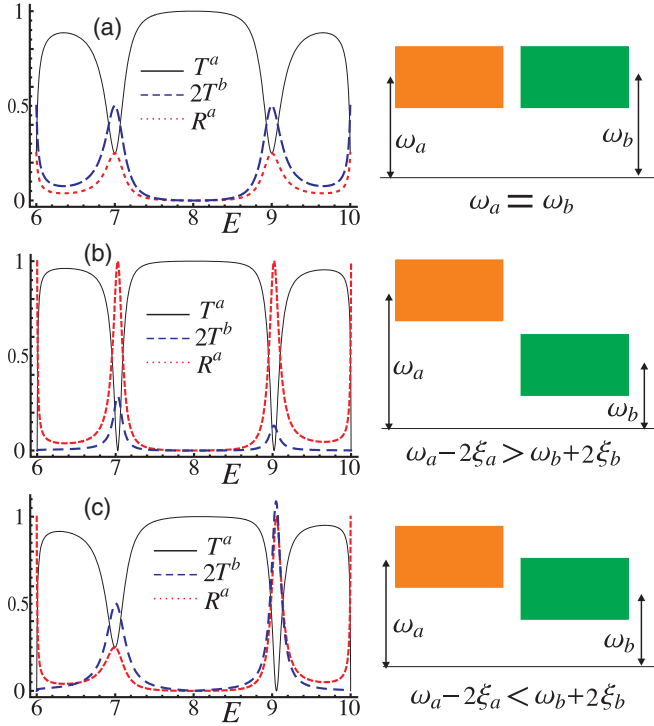
FIG. 2. (Color online) Transmittance $T^a(E)$ (solid black line), reflectance $R^a(E)$ [dotted (red) line], and total transfer rate $2T^b(E)$ [dashed (blue) line] as a function of the energy of the incident wave. (a) $\omega_b = 8$; the two bands of the bare CRWs are maximally overlapped. (b) $\omega_b = 2$; there is no overlap between the two bands. (c) $\omega_b = 6$; the two bands are partially overlapped. For convenience, all the parameters are in units of ξ_a and we always set $\xi_a = \xi_b = 1$, $\omega_a = \omega_E = \omega_S = 8$, $\Omega = 1$, and $g_a = g_b = 0.5$.

(i) the transfer rate does not vanish, and there is no perfect reflection, therefore single photons incident from CRW-a can be transferred to the continuum in CRW-b; and (2) single photons incident from the left side of CRW-a can be totally transmitted to the right side of CRW-a at $E = \omega_S$. We note that the total transmission point cannot be observed in the system studied in Ref. [9]. According to the probability conservation, the incident flux is required to equal the sum of the reflected, transmitted, and transfer fluxes. Hence, the scattering amplitudes satisfy $|t^a|^2 + |r^a|^2 + 2|t^b|^2 = 1$. In Fig. 2(b), there is no overlap between two bands. The total transmission still occurs at vanishing two-photon detuning. However, there are total reflections. It can also be observed that the flow conservation equation is changed as $|t^a|^2 + |r^a|^2 = 1$, which indicates that the photon flow is confined in CRW-a. Actually, these total reflections are caused by the incident energy of a single photon matching the eigenvalues of the bound states of CRW-b with $g_a = 0$. These bound states are local modes around the atom in CRW-b. In Fig. 2(c), there is partial overlap between two bands. The total transmission, total reflection, and transfer to the continuum of CRW-b are all shown in Fig. 2(c). When the energy of the incident photon is out of (within) the overlap region of the two continuum bands, the conservation relation and the related scattering properties are the same as those in Fig. 2(b) [Fig. 2(a)].

IV. COHERENT CONTROL OF SINGLE PHOTONS

In this system, two CRWs provide two 1D continua; each 1D continuum is an open quantum channel for photons. Without the atom, photons incident from one quantum channel cannot transfer to the other. In this section, two band configurations, where energy bands of the CRWs are either maximally overlapped or have no overlap, are considered separately, to better understand how the atom controls the flow of photons.

A. Multichannel quantum router

We first reveal the underlying physics in Fig. 2(a), where two energy bands are overlapped. Two different situations, where the classical driving is turned off or on, are considered.

When the classical driving is turned off (i.e., $\Omega = 0$), single photons incident from one quantum channel (e.g., the CRW-a) will be absorbed by the atom, which transits from its ground state to its excited state. Since the excited state is coupled to a continuum of states, the excited TLS will emit a photon spontaneously into the propagating state of either CRW-a or CRW-b. Consequently, mediated by the atom, photons could be routed from one quantum channel to the other. In other words, the resonant tunneling process of the atomic excited state helps the atom to perform quantum routing. Although it is well known that the spontaneous emission of the excited TLS can be exploited to switch the motion of single photons in a 1D waveguide [6,7], it can also be exploited to redirect the photons coming from one 1D continuum to the other, with the TLS mediating the resonant tunneling process. To study this mechanism, we plot the current flow of the photon in CRW-a and CRW-b in Fig. 3, which are described by the coefficients $T^a(E) + R^a(E)$ and $2T^b(E)$, respectively. The nonvanishing transfer rate around $E = \omega_E$ shows that when the incident energy E approaches the atomic transition energy ω_E, photons coming from one CRW are redirected to the other by resonant tunneling. Actually, the atomic transition energy ω_E determines the position where the minimum flow in CRW-a and the maximum of the probability transferred to CRW-b occur in the energy axis; i.e., the peak transfer rate is centered at $E = \omega_E$. The height of the peak for the transfer rate $2T^b(E)$ takes the maximal value when $g_a = g_b$. The width of the peak for the transfer rate $2T^b(E)$ is determined by the coupling strengths g_a and g_b. The larger the product $g_a g_b$ is, the wider the peak is. The photonic flow can be nearly completely confined in the incident CRW once the incident energy of single photons is largely detuned from the atomic transition energy.

When a classical field is turned on, two dressed states with energies $\omega_\pm$ are created due to the coupling between a pair of well-separated atomic bound levels $|e\rangle$ and $|s\rangle$ and a classical field. These dressed states form doubly excited states of the atom. For an appropriate Rabi frequency, two dressed states are within the energy bands of two CRWs. Single photons coming from CRW-a could excite the atom from its ground states to either of two dressed states, due to the transition driven by cavity mode a_0. The spontaneous emission from the atom provides a chance for photons traveling in both CRWs since the two dressed states are coupled to the continua of both CRWs. These tell us that photons resonantly tunnel from one 1D continuum to the other via two dressed states, which
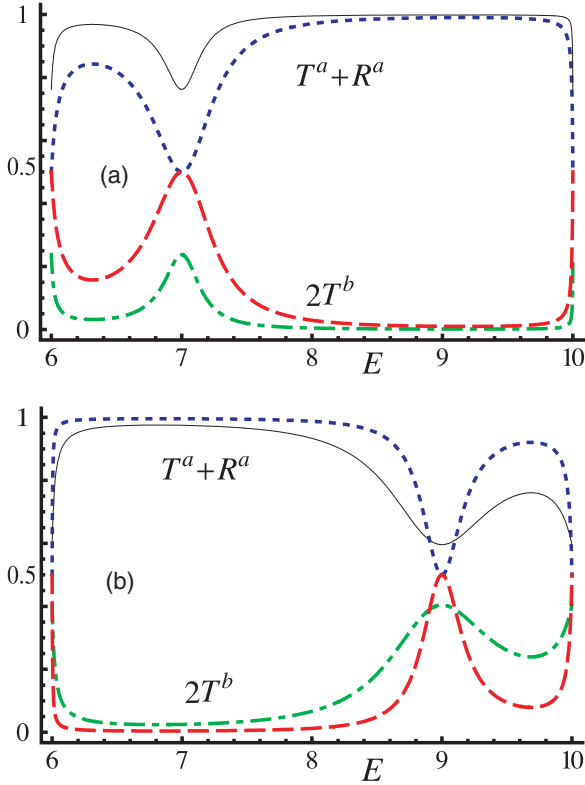
FIG. 3. (Color online) Coefficients $T^a(E) + R^a(E)$ [solid black and dotted (blue) lines], $2T^b(E)$ [dashed (red) and dotted-dashed (green) lines] as a function of the incident photon energy E. The chosen parameters $\xi_a = \xi_b = 1$, $\omega_a = \omega_b = 8$, and $\omega_S = \Omega = 0$ indicate that we study the scattering process for a two-level system interacting with two CRWs, where the energy band of two CRWs overlap. (a) $\omega_E = 7$, $g_a = 0.5$, $g_b = 0.5$ (0.2) for the dotted (blue) and dashed (red) lines [solid black and dotted-dashed (green) lines]. (b) $\omega_E = 9$, $g_a = 0.4$ (0.5), $g_b = 0.4$ (0.8) for the dotted (blue) and dashed (red) lines [solid black and dotted-dashed (green) lines].

fulfills the function of quantum routing. The quantum routing due to the resonant tunneling process via the two dressed states are shown by the two peaks of the transfer rate in Figs. 2(a) and 4. However, differently from the case where the classical field is absent, the photonic flow can be completely confined to the incident CRW, when $E = \omega_S$, as shown in Fig. 4. To determine the direction of the flow in the incident channel, we plot the transmission $T^a(E)$ as a function of the incident energy in Fig. 5. The solid (blue) line [dashed (red) line] is the transmission spectrum when the classical field is turned off (on). It can be found that the classical field makes the solid (blue) line split into a doublet with a separation of 2μ given in Eq. (13), which is the Autler-Townes splitting [40,41]. The transmission coefficient $T^a(E)$, equal to 1 at $E = \omega_S$, indicates that the Autler-Townes splitting yields transparency in a transmission spectrum. Actually, from the point of view of the dressed state [42], the total transmission appearing at the two-photon resonance is the result of the interference between the two resonances via the dressed states.

The above discussion tells us that the atom acts as a multichannel router for single photons, either in the absence or in the presence of a classical field, due to the spontaneous
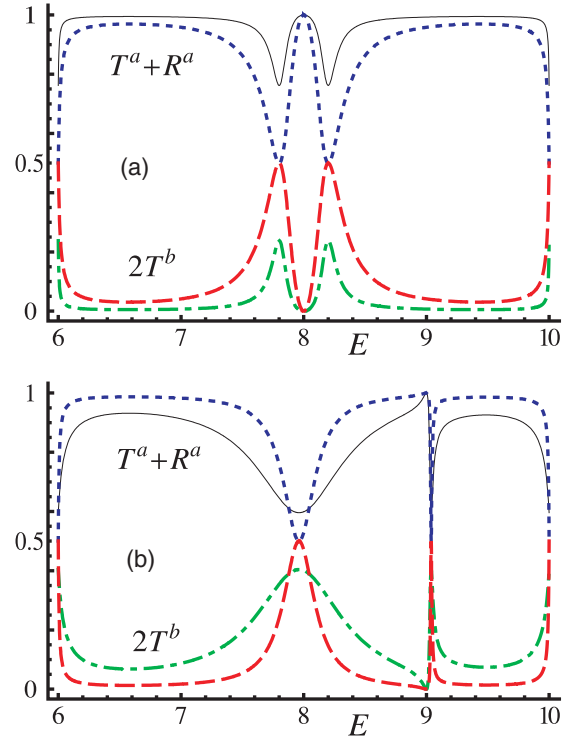

FIG. 4. (Color online) Coefficients $T^a(E) + R^a(E)$ [solid black lines and dotted (blue) lines] and $2T^b(E)$ [dashed (red) and dotted-dashed (green) lines] as a function of the incident photon energy E, when a classical field is applied. Here, the parameters $\xi_a = \xi_b = 1$, $\omega_a = \omega_b = \omega_E = 8$, and $\Omega = 0.2$ are fixed. (a) $\omega_S = 8$, $g_a = 0.5$, $g_b = 0.2$ (0.5) for solid black and dotted-dashed (green) lines [dotted (blue) and dashed (red) lines]. (b) $\omega_S = 9$, $g_a = 0.5$ (0.4), $g_b = 0.8$ (0.4) for solid black and dotted-dashed (green) lines [dotted (blue) and dashed (red) lines].

emission. However, differently from the case where a classical field is absent, the system with an applied classical field exhibits quantum interference between two resonances via the dressed states, which results in the total transmission in the incident channel, when the energy of single photons satisfies the two-photon resonance. Hence a classical field can be used to choose the way single photons will take in this router.
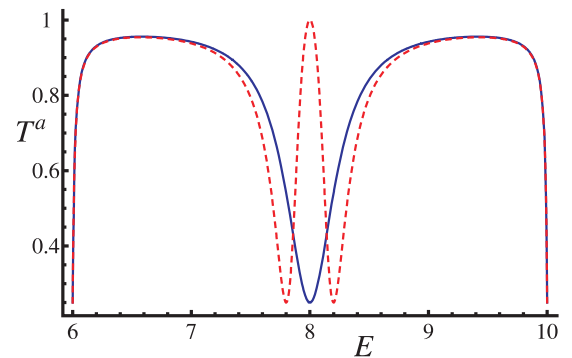

FIG. 5. (Color online) The transmission coefficient T^a in the incident channel versus the energy E of the incident photon. Here, $\omega_S = 0$, $\Omega = 0$ for the solid (blue) line, and $\Omega = 0.2$ for the dashed (red) line. Other parameters are set as follows: $\xi_a = \xi_b = 1$, $\omega_a = \omega_b = \omega_E = \omega_S = 8$, and $g_a = g_b = 0.5$.

B. Single-channel quantum router

We now explore the underlying physical mechanism of perfect reflection in Figs. 2(b) and 2(c). It can be observed in Eq. (15a) that transmission in CRW-a vanishes as long as the condition $2i\xi_b \sin k_b - g_b^2 V(E) = 0$ is satisfied. This condition shows that (i) the parameters related to CRW-b and the atom determine the condition for vanishing transmissions, i.e., the condition is independent of ω_a and g_a, which characterize CRW-a; and (ii) a real k_b cannot meet the condition, and thus the possibility occurs of the complex extension of the wavenumber k_b in CRW-b. Actually, replacing k_b with $(n_b\pi + i\kappa_b)$ yields the condition

$$2\xi_b \exp(in_b\pi) \sinh \kappa_b + g_b^2 V(E_\kappa) = 0 \qquad (16)$$

for the existence of the bound states in CRW-b, where $\kappa_b > 0$ and $n_b = 0, 1$. Here $n_b = 0$ ($n_b = 1$) indicates that the eigenenergies E_κ lie below (above) the band of CRW-b. Bound states appear when the translation invariance of CRW-b is broken. It is the atom coupled to CRW-b which breaks down the translation symmetry of CRW-b.

To demonstrate that Eq. (16) is the condition for the existence of bound states in CRW-b, with a Λ system inside, we begin our study from Eq. (9b). By setting $g_a = 0$, we obtain the discrete-scattering equation for single photons traveling in CRW-b:

$$(E - \omega_b)\beta(j) = -\xi_b [\beta(j-1) + \beta(j+1)]$$
$$+ \delta_{j0}\beta(j) V_b(E). \qquad (17)$$

Since the potential $V_b(E)$ vanishes everywhere except at $j = 0$, the wave function

$$\beta(j) = \begin{cases} D_1 \exp[j(in\pi + \kappa_b)] & \text{for} \quad j < 0, \\ D_2 \exp[j(in\pi - \kappa_b)] & \text{for} \quad j > 0 \end{cases} \qquad (18)$$

must be a damped wave, which decreases exponentially with the distance from the position $j = 0$. Applying the spatial-exponential-decay solution, (18), to Eq. (17) far away from the $j = 0$ point, we obtain the dispersion relation,

$$E = \omega_b - 2\xi_b \exp(in_b\pi) \cosh \kappa_b. \qquad (19)$$

And an even-parity wave function with $D_1 = D_2$ is obtained when applying Eq. (18) to the two sites around the zeroth point of Eq. (17). The condition in Eq. (16) is achieved by inserting the solution, (18), into Eq. (17) at the $j = 0$ point. Using the dispersion relation in Eq. (19), the condition for the existence of bound states in CRW-b can be written in terms of the energy E_κ:

$$(-1)^{n_b}\sqrt{(E_\kappa - \omega_b)^2 - 4\xi_b^2} + g_b^2 V(E_\kappa) = 0. \qquad (20)$$

We note that by letting $\Omega = 0$, Eq. (20) provides the "existence condition" of the bound states in CRW-b with an embedded TLS.

In Fig. 6(a), we solve Eq. (20) in the (Ω, E) plane. It is observed that there are two bound states above the energy band of CRW-b for a nonvanishing Rabi frequency. The energy difference between these two bound states increases as the Rabi frequency increases. And the larger the one-photon detuning $\Delta = \omega_S - \omega_A$ is, the wider the energy difference. Figure 6(b) presents the difference when the classical field is turned on or
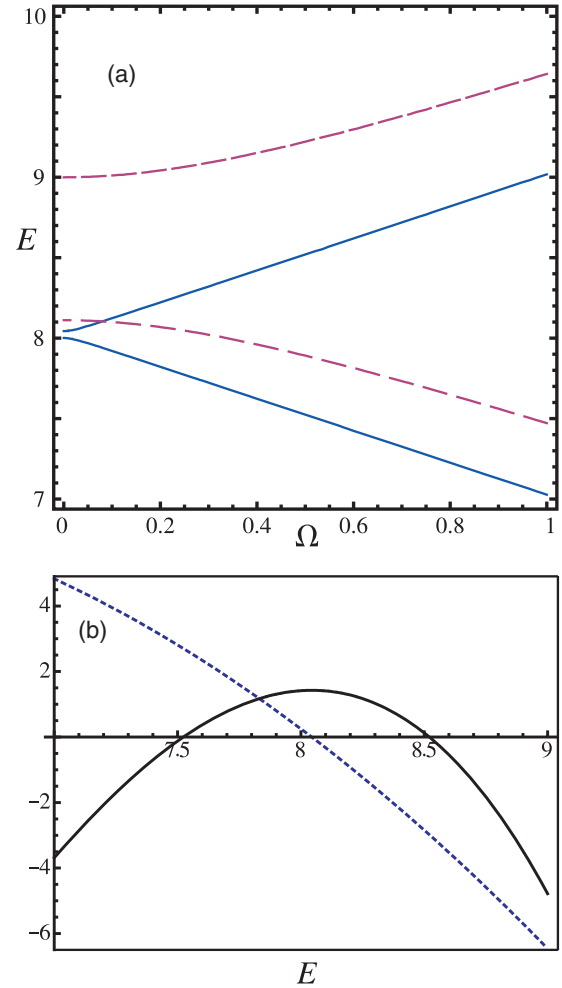

FIG. 6. (Color online) (a) The solution of Eq. (20) in the (Ω, E) plane. $\omega_S = 8$, $g_a = g_b = 0.5$ for the solid (blue) curves, and $\omega_S = 9$, $g_a = 0.5$, $g_b = 0.8$ for the dashed (red) curves. (b) Left side of Eq. (20) ($n_b = 1$) as a function of the energy with $g_a = g_b = 0.5$. The points along the transverse axis indicate the energy of the bound state when $\omega_S = 0$, $\Omega = 0$ for the dashed (blue) curve and $\omega_S = 8$, $\Omega = 0.5$ for the solid black line. In there figures, we have chosen $\omega_a = 8$ and $\omega_b = 2$.

off. There is only one bound state localized around the TLS when $\Omega = 0$. It is shown in Fig. 6(b) that the energies of these two bound states are not the energies $\omega_\pm$ of the two dressed states. In Fig. 7, we plot the transfer rate $T^b(E)$ as a function of the energy E, to show the difference between the absence and the presence of a classical field. It can be observed that the applied classical field splits the bound state above the band into two.

In Figs. 2(b) and 7, bound states of CRW-b are degenerate in energy with the continuum of CRW-a. It is the coupling between bound states in CRW-b and the continuum in CRW-a which leads to the observation of bound states via the scattering process. For single photons incident from CRW-a, the continuum of CRW-a provides an open channel for the propagation of photons; bound states, on the other hand, provide closed channels. When the energy of the incident photon matches either of the bound states, the interference between the open and the closed channels leads to the total reflection of
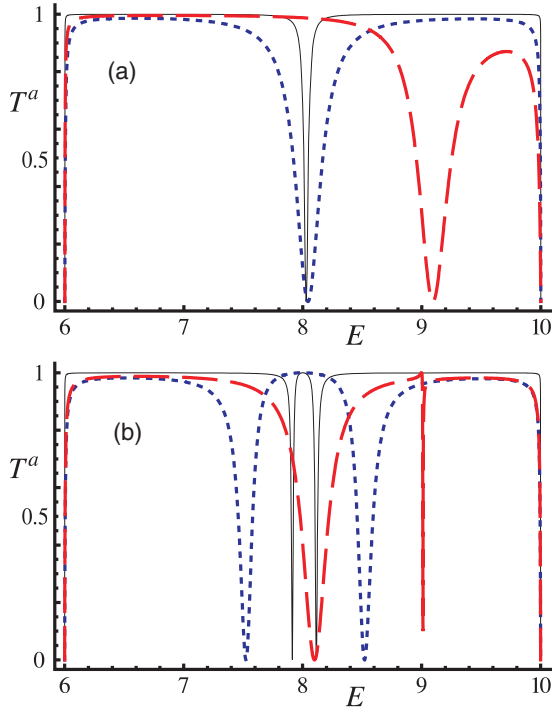
FIG. 7. (Color online) Transmission coefficient $T^a(E)$ as a function of the energy E when a classical field is turned off (a) and on (b). (a) $\omega_A = 8$, $g_a = 0.2$, $g_b = 0.4$ for the solid black line; $\omega_A = 8$, $g_a = 0.5$, $g_b = 0.5$ for the dotted (blue) line; and $\omega_A = 9$, $g_a = 0.5$, $g_b = 0.8$ for the dashed (red) line. (b) $\omega_A = 8$, $\Omega = 0.1$, $g_a = 0.2$, $g_b = 0.4$ for the solid black line; $\omega_A = 8$, $\Omega = 0.5$, $g_a = 0.5$, $g_b = 0.5$ for the dotted (blue) line; and $\omega_A = 9$, $\Omega = 0.1$, $g_a = 0.5$, $g_b = 0.8$ for the dashed (red) line. Throughout, we have set $\omega_a = 8$ and $\omega_b = 2$.

single photons. We note that the mechanism of these total reflections is different from the coherent interference between the incoming wave and the wave emitted by the doubly dressed states.

For the band configuration in Fig. 2(b), the motion of single photons from one CRW is confined to the incident CRW. In this case, the atom functions as a single-photon switch, which routes photons forward or backward in the incident quantum channel. The scattering process is similar to the Feshbach resonance in cold-atom scattering, where the scattering cross section diverges when the energy of the incident particle matches the bound state of the closed channel.

C. Localized photons for the entire system

Solutions to Eqs. (9) can be found in the form of either (i) a superposition of extended propagating Bloch waves (incident reflected, transmitted, and transferred by the atom embedded in the CRWs) or (ii) localized states around the location of the atom. We note that these localized states are eigenstates of the total system different from the one obtained above. To show the possibility of a bound state of the total system, we now consider the case where two bands of CRWs do not overlap. Our purpose here is to derive the condition for the existence of bound states. The bound state now is assumed to have the following solutions with even parity:

$$\alpha_\kappa(j) = \begin{cases} D \exp\left[j\,(in_a\pi + \kappa_a)\right] & \text{for} \quad j < 0, \\ D \exp\left[j\,(in_a\pi - \kappa_a)\right] & \text{for} \quad j > 0, \end{cases} \quad (21)$$

$$\beta_\kappa(j) = \begin{cases} C \exp\left[j\,(in_b\pi + \kappa_b)\right] & \text{for} \quad j < 0, \\ C \exp\left[j\,(in_b\pi - \kappa_b)\right] & \text{for} \quad j > 0, \end{cases} \quad (22)$$

which are localized around the zeroth site, where the atom is embedded. Applying the assumed solution to Eq. (17) far away from the $j = 0$ point, we find that κ_a, and κ_b are related to each other via the energy

$$E_\kappa = \omega_a - (-1)^{n_a}2\xi_a \cosh\kappa_a = \omega_b - (-1)^{n_b}2\xi_b \cosh\kappa_b. \quad (23)$$

Applying the assumed solution to Eq. (17) at the $j = 0$ point yields the final condition for the existence of the bound state in the total system,

$$G^2(E) = \prod_d [(-1)^{n_d}2\xi_d \sinh\kappa_d + V_d(E)], \quad (24)$$

which is the denominator of Eq. (15) with k_d replaced by $n_d\pi + i\kappa_d$, where $d = a,b$. Bound states of the total system provide no contribution to the quantum transport in the one-quantum subspace, because scattering states survive only inside the band.

V. CONTROLLABLE AND SCATTERING-FREE CHANNELS

In the above discussion, single photons are incident from one quantum channel. We found that the resonant tunneling process transfers single photons from one quantum channel to the other when two bands overlap. In this section, we focus on the overlap band configuration shown at the right in Fig. 2(a). The purpose now is to investigate the quantum interference among different quantum channels and to find the function of the atom for waves incident from two quantum channels.

We now begin our discussion from the Hamiltonian H_R in the rotating frame. We first introduce the bright (B_j) and dark (D_j) modes,

$$B_j = a_j\cos\theta + b_j\sin\theta, \quad (25a)$$

$$D_j = a_j\sin\theta - b_j\cos\theta, \quad (25b)$$

which are a linear combination of the cavity-mode operators of both CRWs. Here, $\tan\theta = g_b/g_a$. In terms of the bright and dark operators and the condition $\omega_a = \omega_b = \omega$, $\xi_a = \xi_b = \xi$ for an overlap band configuration, the Hamiltonian of the system reads

$$H_R = \sum_j [\omega B_j^\dagger B_j - \xi(B_{j+1}^\dagger B_j + \text{H.c.})]$$

$$+ \sum_j [\omega D_j^\dagger D_j - \xi(D_{j+1}^\dagger D_j + \text{H.c.})]$$

$$+ H_A + g|e\rangle\langle g|B_0 + \Omega|e\rangle\langle s| + \text{H.c.}, \quad (26)$$

where H_A is given in Eq. (5) and the coupling strength $g \equiv \sqrt{g_a^2 + g_b^2}$. Two virtual CRWs (the bright and dark CRWs) provide the propagating state for single photons. For convenience, the CRW described by operator B_j (D_j) is called
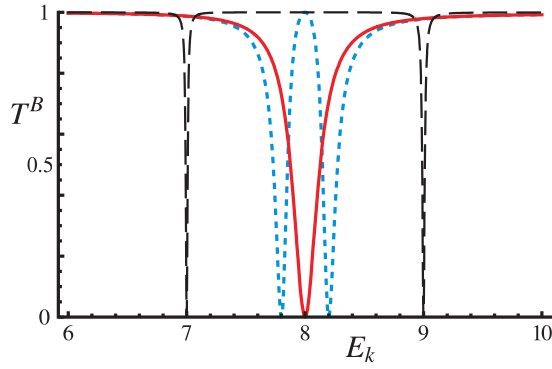
FIG. 8. (Color online) The transmission coefficient $T^B \equiv |t^B|^2$ as a function of the energy E_k. We set $\xi = 1$, $\omega = \omega_E = \omega_S = 8$, $\Omega = 0.2$, $g = 0.5$ for the dotted (blue) line, $\Omega = 0$, $g = 0.5$ for the solid (red) line, and $\Omega = 1$, $g = 0.2$ for the dashed black line.

the bright (dark) CRW, and the quantum channel constructed by the bright (dark) CRW is called the bright (dark) channel. The dark CRW is decoupled from the atom. Consequently, the dark channel is a scattering-free channel; i.e., single photons incident from the left in the dark CRW are transmitted into the right with unit probability. However, single photons incident from the bright CRW could be absorbed by the atom and later emitted spontaneously into the bright CRW, leading to left-going and right-going photons. This process is described by a wave with energy $E_k = \omega - 2\xi \cos k$, incident from the left side of the bright CRW, that results in a reflected and transmitted wave in the same CRW.

By the same approach as in Sec. III, the transmission amplitude is obtained as

$$t^B = \frac{2i\xi \sin k}{2i\xi \sin k - g^2 V(E_k)}, \qquad (27)$$

where $V(E_k)$ is given in Eq. (10). And the reflection amplitude r_B is related to t_B by $t_B = r_B + 1$. In Fig. 8, we plot the transmission coefficient as a function of the incident energy. It can be found that (i) when $\Omega = 0$, single photons can be totally reflected when their incident energy is resonant with the atomic transition $|e\rangle \leftrightarrow |g\rangle$; and (ii) when $\Omega \neq 0$, single photons have a probability $T^B = 1$ of being transmitted when the incident energy satisfies the two-photon resonance $E_k = \omega_S$ and a probability $R^B \equiv |r^B|^2 = 1$ of being reflected when the incident energy matches the energy $\omega_\pm$ of the dressed states. These total reflections are caused by the quantum interference between the spontaneous emission from the atom and the propagating modes in the 1D continuum. The waves emitted by the doubly dressed states interfere coherently, such that the back-traveling wave is eliminated while the forward wave is constructed, which leads to the perfect transmission of the incident photon. The transmission spectra at $\Omega = 0$ and $\Omega \neq 0$ indicate that the atom is transparent once the classical field is applied. Hence, we can control the reflection and transmission by tuning the Rabi frequency and the classical-field frequency for waves incident from the bright CRW. Hence, we denote the bright channel as the controllable channel. It should be noted that the propagating states of the bright channel are orthogonal to those of the dark channel.

VI. DISCUSSION AND CONCLUSION

We have studied the coherent scattering process of single photons in two 1D CRWs. The scattering target is a Λ-type atom possessing an inversion center, which fulfills the quantum routing of single photons due to quantum interference.

When there is an overlap between two bands of the CRWs, the resonant tunneling process induces the atom to act as a multichannel router. When a classical field is absent, one can turn on the multichannel routing by adjusting the transition frequency of the atom between state $|e\rangle$ and state $|g\rangle$ to match the desired propagating states of both CRWs. To turn off the multichannel routing, one has to tune the atomic transition energy far away from the energy of the incident photons. Obviously, the closure of the multichannel routing based on large detuning is not perfect. To perfectly turn off the quantum routing, one can utilize the Autler-Townes splitting. The procedure is as follows: first, apply a classical field to drive the transition between the excited state of the atom and an intermediate level, then adjust the frequency and the intensity of the classical field. In addition, the scatter-free and controllable channels are found for waves incident from both CRWs. Single photons propagate freely in the scatter-free channel. Without a classical field, the atom acts only as a perfect mirror for incident waves in the controllable channel due to the Fano resonance. With a classical field applied, the atom acts not only as a perfect mirror but also as a transparent medium; i.e., the classical field selects the photon which is transmitted or reflected.

When there is no overlap between the two bands, the coupling between discrete energy levels and a continuum makes the atom act as a single-channel router. When the classical field is absent, the single-channel router is turned on by adjusting the atomic transition frequency between state $|e\rangle$ and state $|g\rangle$, so that the bound state in one CRW matches the incident energy of the other CRW. To turn off the single-channel router, one has to adjust the atomic transition frequency ω_E so that the bound states of the CRW are far away from the other CRW. However, this mechanism for turning off the single-channel router is not perfect. With a classical field applied, one not only can shift the transmission zeros so that the single-channel router can be operated at different energies, but also can completely turn off the single-channel router for single photons with a given energy.

[1] H. J. Kimble, Nature (London) **453**, 1023 (2008).

[2] M. A. Hall, J. B. Altepeter, and P. Kumar, Phys. Rev. Lett. **106**, 053901 (2011).

[3] K. Lemr and A. Černoch, Opt. Commun. **300**, 282 (2013).

[4] K. Lemr, K. Bartkiewicz, A. Černoch, and J. Soubusta, Phys. Rev. A **87**, 062333 (2013).

[5] X.-Y. Chang, Y.-X. Wang, C. Zu, K. Liu, and L.-M. Duan, arXiv:1207.7265.

[6] J. T. Shen and S. Fan, Phys. Rev. Lett. **95**, 213001 (2005); Opt. Lett. **30**, 2001 (2005).

[7] L. Zhou, Z. R. Gong, Y.-x. Liu, C. P. Sun, and F. Nori, Phys. Rev. Lett. **101**, 100501 (2008).

[8] L. Zhou, H. Dong, Y.-x. Liu, C. P. Sun, and F. Nori, Phys. Rev. A **78**, 063827 (2008); Z. R. Gong, H. Ian, L. Zhou, and C. P. Sun, *ibid.* **78**, 053806 (2008).

[9] L. Zhou, L. P. Yang, Y. Li, and C. P. Sun, Phys. Rev. Lett. **111**, 103604 (2013).

[10] L. Zhou, Y. Chang, H. Dong, L. M. Kuang, and C. P. Sun, Phys. Rev. A **85**, 013806 (2012).

[11] C.-H. Yan, L.-F. Wei, W.-Z. Jia, and J.-T. Shen, Phys. Rev. A **84**, 045801 (2011).

[12] M.-T. Cheng, X.-S. Ma, M.-T. Ding, Y.-Q. Luo, and G.-X. Zhao, Phys. Rev. A **85**, 053840 (2012).

[13] Q. Li, L. Zhou, and C. P. Sun, arXiv:1308.2011.

[14] J. T. Shen and S. Fan, Phys. Rev. Lett. **98**, 153003 (2007).

[15] P. Longo, P. Schmitteckert, and K. Busch, Phys. Rev. Lett. **104**, 023602 (2010); Phys. Rev. A **83**, 063828 (2011).

[16] M. Alexanian, Phys. Rev. A **81**, 015805 (2010).

[17] T. Shi and C. P. Sun, Phys. Rev. B **79**, 205111 (2009); T. Shi, S. Fan, and C. P. Sun, Phys. Rev. A **84**, 063803 (2011); T. Shi and S. Fan, *ibid.* **87**, 063818 (2013).

[18] H.-X. Zheng, D. J. Gauthier, and H. U. Baranger, Phys. Rev. A **82**, 063816 (2010); Phys. Rev. Lett. **107**, 223601 (2011); Phys. Rev. A **85**, 043832 (2012); Phys. Rev. Lett. **111**, 090502 (2013).

[19] D. Roy, Phys. Rev. Lett. **106**, 053601 (2011); Phys. Rev. B **81**, 155117 (2010); Phys. Rev. A **83**, 043823 (2011).

[20] E. Rephaeli and S. Fan, Phys. Rev. Lett. **108**, 143602 (2012).

[21] W. B. Yan, Q. B. Fan, and L. Zhou, Phys. Rev. A **85**, 015803 (2012).

[22] P. Longo, J. H. Cole, and K. Busch, Opt. Express **20**, 12326 (2012).

[23] A. V. Akimov, A. Mukherjee, C. L. Yu, D. E. Chang, A. S. Zibrov, P. R. Hemmer, H. Park, and M. D. Lukin, Nature (London) **450**, 402 (2007).

[24] T. Aoki, A. S. Parkins, D. J. Alton, C. A. Regal, B. Dayan, E. Ostby, K. J. Vahala, and H. J. Kimble, Phys. Rev. Lett. **102**, 083601 (2009).

[25] M. Bajcsy, S. Hofferberth, V. Balic, T. Peyronel, M. Hafezi, A. S. Zibrov, V. Vuletic, and M. D. Lukin, Phys. Rev. Lett. **102**, 203902 (2009).

[26] T. M. Babinec, B. J. M. Hausmann, M. Khan, Y. Zhang, J. R. Maze, P. R. Hemmer, and M. Lončar, Nat. Nanotechnol. **5**, 195 (2010).

[27] O. V. Astafiev, A. M. Zagoskin, A. A. Abdumalikov, Jr., Y. A. Pashkin, T. Yamamoto, K. Inomata, Y. Nakamura, and J. S. Tsai, Science **327**, 840 (2010); O. V. Astafiev, Y. A. Pashkin, Y. Nakamura, J. S. Tsai, A. A. Abdumalikov, and A. M. Zagoskin, Phys. Rev. Lett. **104**, 183603 (2010).

[28] J. Claudon, J. Bleuse, N. S. Malik, M. Bazin, P. Jaffrennou, N. Gregersen, C. Sauvan, P. Lalanne, and J. M. Gérard, Nat. Photon. **4**, 174 (2010); J. Bleuse, J. Claudon, M. Creasey, N. S. Malik, J. M. Gerard, I. Maksymov, J. P. Hugonin, and P. Lalanne, Phys. Rev. Lett. **106**, 103601 (2011).

[29] A. Laucht, S. Pütz, T. Günthner, N. Hauke, R. Saive, S. Frédérick, M. Bichler, M.-C. Amann, A. W. Holleitner, M. Kaniber, and J. J. Finley, Phys. Rev. X **2**, 011014 (2012).

[30] I. C. Hoi, C. M. Wilson, G. Johansson, T. Palomaki, B. Peropadre, and P. Delsing, Phys. Rev. Lett. **107**, 073601 (2011); I. C. Hoi, T. Palomaki, J. Lindkvist, G. Johansson, P. Delsing, and C. M. Wilson, *ibid.* **108**, 263601 (2012).

[31] M. J. Hartmann, F. G. S. L. Brandão, and M. B. Plenio, Laser Photon. Rev. **2**, 527 (2008).

[32] M. Notomi, E. Kuramochi, and T. Tanabe, Nat. Photon. **2**, 741 (2008).

[33] L. Zhou, S. Yang, Y.-x. Liu, C. P. Sun, and F. Nori, Phys. Rev. A **80**, 062109 (2009).

[34] P. Král and M. Shapiro, Phys. Rev. Lett. **87**, 183002 (2001); P. Král, Z. Amitay, and M. Shapiro, *ibid.* **89**, 063002 (2002); P. Král, I. Thanopulos, M. Shapiro, and D. Cohen, *ibid.* **90**, 033001 (2003); I. Thanopulos, P. Král, and M. Shapiro, *ibid.* **92**, 113003 (2004); P. Král, I. Thanopulos, and M. Shapiro, Phys. Rev. A **72**, 020303(R) (2005).

[35] Y. Li, L. Zheng, Y.-x. Liu, and C. P. Sun, Phys. Rev. A **73**, 043805 (2006).

[36] Y.-x. Liu, J. Q. You, L. F. Wei, C. P. Sun, and F. Nori, Phys. Rev. Lett. **95**, 087001 (2005).

[37] Y. Li, C. Bruder, and C. P. Sun, Phys. Rev. Lett. **99**, 130403 (2007).

[38] C. E. Creffield, Phys. Rev. Lett. **99**, 110501 (2007).

[39] D. Zueco, F. Galve, S. Kohler, and P. Hänggi, Phys. Rev. A **80**, 042303 (2009).

[40] S. H. Autler and C. H. Townes, Phys. Rev. **100**, 703 (1955).

[41] H. Ian, Y.-x. Liu, and F. Nori, Phys. Rev. A **81**, 063823 (2010).

[42] M. Fleischhauer, A. Imamoglu, and J. P. Marangos, Rev. Mod. Phys. **77**, 633 (2005).